

Contents lists available at [ScienceDirect](http://www.sciencedirect.com)

Chemical Engineering Research and Design

journal homepage: www.elsevier.com/locate/cherd

IChemE



Experimental design and batch experiments for optimization of Cr(VI) removal from aqueous solutions by hydrous cerium oxide nanoparticles

Ahmad B. Albadarin^{a,*}, Zheyu Yang^a, Chirangano Mangwandi^a,
Yoann Glocheux^a, Gavin Walker^{a,b}, M.N.M. Ahmad^{a,c}

^a School of Chemistry and Chemical Engineering, Queen's University Belfast, Northern Ireland, UK

^b Materials Surface Science Institute, Department of Chemical and Environmental Sciences, University of Limerick, Ireland

^c Chemical Engineering, Faculty of Engineering and Architecture, American University of Beirut, Lebanon

A B S T R A C T

Hydrous cerium oxide (HCO) was synthesized by intercalation of solutions of cerium(III) nitrate and sodium hydroxide and evaluated as an adsorbent for the removal of hexavalent chromium from aqueous solutions. Simple batch experiments and a 2⁵ factorial experimental design were employed to screen the variables affecting Cr(VI) removal efficiency. The effects of the process variables; solution pH, initial Cr(VI) concentration, temperature, adsorbent dose and ionic strength were examined. Using the experimental results, a linear mathematical model representing the influence of the different variables and their interactions was obtained. Analysis of variance (ANOVA) demonstrated that Cr(VI) adsorption significantly increases with decreased solution pH, initial concentration and amount of adsorbent used (dose), but slightly decreased with an increase in temperature and ionic strength. The optimization study indicates 99% as the maximum removal at pH 2, 20 °C, 1.923 mM of metal concentration and a sorbent dose of 4 g/dm³. At these optimal conditions, Langmuir, Freundlich and Redlich–Peterson isotherm models were obtained. The maximum adsorption capacity of Cr(VI) adsorbed by HCO was 0.828 mmol/g, calculated by the Langmuir isotherm model. Desorption of chromium indicated that the HCO adsorbent can be regenerated using NaOH solution 0.1 M (up to 85%). The adsorption interactions between the surface sites of HCO and the Cr(VI) ions were found to be a combined effect of both anion exchange and surface complexation with the formation of an inner-sphere complex.

Crown Copyright © 2013 Published by Elsevier B.V. on behalf of The Institution of Chemical Engineers. All rights reserved.

Keywords: Chromium; Adsorption isotherm; Nanoparticles; Optimization; Hydrous cerium oxide; Desorption

1. Introduction

Wastewater contaminations have led to the development of practical and cost effective adsorption processes for the detoxification of various pollutants (Duffy et al., 2006). Inorganic elements occurring in various oxidation states are a specific type of impurity, as they often have different degrees of toxicity depending on the particular oxidation state (Fendorf, 1995). Two common oxidation states of chromium

(Cr(III) and Cr(VI)) are present in the environment, and their physicochemical properties are each drastically different from those of the other (Kotas and Stasicka, 2000; Albadarin et al., 2012a). The interest in Cr(VI) removal originates from widespread use of this metal in various industries such as metallurgical (steel, ferro- and nonferrous alloys), chemical (pigments, electroplating, tanning and other) and refractories (chrome and chrome-magnesite) (Kotas and Stasicka, 2000). Excessive quantities of Cr compounds are discharged

* Corresponding author. Tel.: +44 07787540865.

E-mail addresses: aalbadarin01@qub.ac.uk, ahmad.albadarin@qub.ac.uk (A.B. Albadarin).

Received 20 June 2013; Received in revised form 7 October 2013; Accepted 15 October 2013

in liquid, solid, and gaseous wastes into the environment and can ultimately have significant adverse biological and ecological effects (Zou et al., 2006). Cr(VI) is approximately 100 times more toxic and 1000 times more mutagenic than Cr(III), which is known to be indispensable for animal nutrition (Iaska et al., 2012; Albadarin et al., 2012b). Aqueous complexes of Cr(VI) have been the object of attentive investigation mainly due to their toxicity as a potential carcinogen, causing damage to DNA (Albadarin et al., 2012a; McCarroll et al., 2010). As an economical and efficient method for the removal of Cr(VI) from aqueous solution, adsorption has been extensively applied. Simple and cost effective adsorbents such as; activated carbon, coconut coir pith, wheat residue derived black and biochar are known for their efficiency in the adsorption of chromium (Santhana Krishna Kumar et al., 2012). Nanotechnology is the engineering of functional systems at the molecular scale, which offer new products and process alternatives for water purification, the advantage being that these materials have a large surface to volume ratio (Recillas et al., 2010; Al-Degs et al., 2008). In recent years, synthesized nano-sized adsorbents, such as iron nanoparticles decorated grapheme (Jabeen et al., 2011), CeO₂ nano-crystal microspheres (Xiao et al., 2009) and diatomite-supported/unsupported magnetite nanoparticles (Yuan et al., 2010) had been extensively studied and demonstrate promising results for Cr(VI) removal from aqueous environment.

Cerium oxide, because of its specific physical and chemical properties, has been widely studied in catalysts, UV shielding materials, electrolyte materials of solid oxide fuel cells and chemical mechanical planarization materials (Li et al., 2012). Cerium oxide has the lowest solubility in acidic media among the rare earth metal oxides, and does not elute during the removal of harmful ions in aqueous solutions. Therefore, cerium oxide is assumed to be one of the more encouraging conventional adsorbents for removing hazardous anions. In many environmental remediation applications, cerium oxide had shown a high adsorption capacity for various anions, for instance; fluoride (Raichur and Jyoti Basu, 2001), arsenic (Li et al., 2012) and bichromate (Xiao et al., 2009). Moreover, efficient and less costly fixed bed adsorbents including nanomaterials used as adsorbents could remove Cr(VI) ions from wastewater during municipal treatment or in point of use applications (Duranoğlu et al., 2012).

An earlier study reported by Recillas et al. (2010) for the adsorption of Cr(VI) onto cerium oxide, important parameters influencing the adsorption process such as pH, ionic strength, and temperature were not examined. Moreover, no systematic reports presently exist on the hydrous cerium oxide removal of Cr(VI), and Cr(VI) adsorption mechanism studies using this material are scarce. Here we report a comprehensive investigation of Cr(VI) ions adsorption by hydrous cerium oxide (HCO) nanoparticles under various experimental conditions based on a two-part study. Initially, a X^Y factorial design with central points was utilized for optimization studies. Then, the influence of solution pH, initial Cr(VI) concentration, equilibrium isotherms, adsorbent dose, presence of other ions and desorption in batch systems was studied for further detailed discussions. This study focuses on the influence of altering the conditions for removal of chromium(VI) using nanoparticle materials; especially those which have not been clearly investigated before.

2. Experimental and analytical methods

2.1. Chemicals and materials

All chemicals were reagent grade and used without further purification. Potassium dichromate, K₂Cr₂O₇ (Fisher scientific >99.5%) was used to prepare Cr(VI) stock solution. Nitric acid (65–68%) and sodium hydroxide were used for the pH adjustment. Sodium nitrate was used in the ionic strength experiment. NaCl, KNO₃, NH₄NO₃, K₂SO₄, (NH₄)₃PO₄, MgSO₄ salts were used in the competing ions experiment. NaOH powder, cerium(III) nitrate hexahydrate, Ce(NO₃)₃·6H₂O (Sigma–Aldrich UK) and absolute ethanol were used to prepare the hydrous cerium oxide nanoparticles.

2.2. Methods

2.2.1. Preparation of hydrous cerium oxide

Hydrous cerium oxide nanoparticles denoted as HCO were synthesized by the precipitation method described by Li et al. (2012). Two different solutions with 0.2 M NaOH and 0.05 M Ce(NO₃)₃·6H₂O concentrations were prepared by dissolving a certain amount of NaOH and Ce(NO₃)₃·6H₂O powder in absolute ethanol. Solutions were then vigorously mixed in air using a hot plate stirrer for 20 min at room temperature. After mixing for 20 min, bright yellow precipitates were formed and then collected by filtration, washed several times with deionised water and absolute ethanol, dried at 110 °C for 12 h and ground manually into a fine powder.

2.2.2. Characterization of hydrous cerium oxide nanoparticles

BET surface area of HCO nanoparticles was measured using a Nova 4200e surface area analyser from Quantachrome instruments. Samples were degassed for 16 h at 60 °C under vacuum and analyzed at 77 K under nitrogen. The functional groups of the HCO before and after Cr(VI) adsorption were examined using a FT-IR Spectrometer (PerkinElmer Spectrum 100 spectrophotometer). A sample which was in contact with a Cr(VI) solution of C₀ = 1.923 mM and pH 2 for 4 days was selected. Samples were homogeneously milled to a fine powder with anhydrous potassium bromide in a ratio of 1/20. The powder was then compacted under a pressure of 8000 kg/cm² to form a translucent disc. All the data was measured in the spectral range 4000–400 cm⁻¹.

2.2.3. Adsorbate solution

An aqueous stock solution of 19.23 mM Cr(VI) was prepared by dissolving 2.825 g of K₂Cr₂O₇ in 1 dm³ of deionised water (18.0 mΩ cm supplied by a Millipore Milli-Q system). Cr(VI)-bearing solutions were freshly prepared by diluting the stock solution to given desired concentrations with deionised water.

2.2.4. Experimental design for optimization

A 2⁵ factorial design of experiments with central points was used to investigate the effects of the independent process variables and their interactions on Cr(VI) removal efficiency. The selected independent factors were; solution pH, initial Cr(VI) concentration, temperature, adsorbent dose and ionic strength. The ranges and the levels of the variables studied in this research are pH (2, 5), initial concentration C₀ (0.384, 1.923 mM), temperature (20, 65 °C) adsorbent dose (0.025, 0.10 g) and ionic strength (0.05, 0.15 M).

2.3. Adsorption from solution

All laboratory glassware were washed with deionised water after being soaked in a HNO₃ (10%, v/v) bath overnight. The pH of various suspensions was adjusted throughout the experiment by adding either 0.05 M HNO₃ or NaOH. During the adsorption experiment, all the suspensions were put in glass jars and firmly sealed and agitated at 100 rpm using mechanical shaker GerhardT type for 24 h at room temperature. After the adsorption, the suspensions were filtered for Cr(VI) concentration analysis. Cr(VI) concentration in the supernatant was measured spectrophotometrically on a HACH metre (Davidson & Hardy LTD, DR2800) (at wavelength, $\lambda = 540$ nm) using the diphenylcarbazide method described in (Albadarin et al., 2012a). The total Cr samples were analyzed by inductive coupled plasma (ICP-OES, Optima 4300 DV, Perkin Elmer, USA) at wavelength 283.5 nm using Argon gas as the fuel. All experiments were carried out in duplicate and average values were reported. The standard error was less than 5%. The Cr(VI) synthetic solution adsorption studies were completed by the following conditions.

2.3.1. Contact time study

Solution pH 2; initial Cr(VI) concentrations 0.384, 1.538, 2.692, 3.846 mM; shaking time 4 days at 100 rpm; hydrous cerium oxide dose 4 g/dm³; T = 20 °C.

2.3.2. Effect of pH

Solution pH 2–10; initial Cr(VI) concentrations 0.769 and 1.923 mM; shaking time 4 days at 100 rpm; hydrous cerium oxide dose 4 g/dm³; T = 20 °C.

2.3.3. Effect of adsorbent dose

Hydrous cerium oxide dose 1–6 g/dm³; solution pH 2; initial Cr(VI) concentrations 1.923 mM; shaking time 4 days at 100 rpm; T = 20 °C.

2.3.4. Effect of co-existing anions

Salt: 0.1 M NaCl, KNO₃, NH₄NO₃, K₂SO₄, (NH₄)₃PO₄, MgSO₄; solution pH 2; initial Cr(VI) concentrations 1.923 mM; shaking time 4 days at 100 rpm; hydrous cerium oxide dose 4 g/dm³; and T = 20 °C.

2.3.5. Adsorption isotherms

Solution pH 2; initial Cr(VI) concentrations 0.384–3.846 mM; shaking time 4 days at 100 rpm; hydrous cerium oxide dose 4 g/dm³; T = 20 °C.

2.3.6. Desorption studies

Finally, for desorption studies, hydrous cerium oxide corresponding to 0.2 g dry adsorbent was mixed with 50 cm³ Cr(VI) solution (1.923 mM). After 120 h adsorption, the adsorbent was separated and dried overnight at 110 °C. The spent adsorbent was then put in contact with 50 cm³ of different desorbent solutions: deionized water, H₂SO₄, NaOH and HCl and then agitated for time periods no longer than the equilibrium time. Percentage desorption was calculated as:

Desorption(%)

$$= \frac{\text{amount of Cr(VI) ions desorbed to the desorption medium}}{\text{amount of Cr(VI) ions adsorbed onto the HCO}} \times 100\% \quad (1)$$

2.4. Apparent capacity measurements

The method of concentration difference between the initial concentration, C₀ (mM) and equilibrium concentration, C_e (mM), was used to calculate the Cr(VI) uptake, q_e (mmol/g), and percentage removal (%), as shown below:

$$q_e = \left[\frac{C_0 - C_e}{M} \right] \times V \quad (2)$$

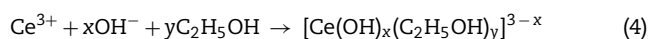
$$\text{Percentage removal(\%)} = \left[1 - \frac{C_e}{C_0} \right] \times 100\% \quad (3)$$

where M is the mass of HCO used (g) and V is the volume of the solution (dm³).

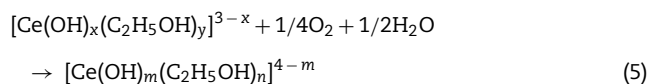
3. Results and discussion

3.1. HCO adsorbent characterization

The preparation of HCO nanoparticles was carried out by interacting Ce(NO₃)₃·6H₂O and NaOH in ethanol. During the reaction, the colour of the reaction suspension changed from dark brown to bright yellow within 20 min of mixing. The above colloidal precipitates were thought to be polymers of cerium hydroxide coordinated with ethanol through the following reactions (Zhang et al., 2003):



The chemical valence of cerium in the precipitation has changed from Ce³⁺ to Ce⁴⁺ which was preferred in high base solution. The Ce³⁺/Ce⁴⁺ transfer process can be expressed by the following equation:



The HCO nanoparticles BET surface specific area was determined as 187 m²/g. The HCO surface area is bigger than that for hydrous titanium oxide 185 m²/g (Tel and Altas, 2004), magnetite nanoparticles 86.6 m²/g (Yuan et al., 2010) and aluminium oxide 78.1 m²/g (Álvarez-Ayuso et al., 2007) from the reported literature data for Cr(VI) removal. The crystallite size of HCO nanoparticles was previously determined as 3.7 nm using X-ray diffraction (Li et al., 2012).

3.2. Statistical design of experiments

The parameters involved in the adsorption experiments were optimized by full factorial design. An empirical model was fitted to the experimental data and a summary of the fit and errors of the factorial model are presented in Table 1. Table 1 shows that initial concentration (B), dose (D) and pH (A) of the solution are the most significant variables on the removal of Cr(VI); the interaction terms AB, AC and BD are also significant.

The model for the adsorption of Cr(VI) is described by;

$$q_e = 0.52227 - 0.13091 \times A + 0.64684 \times B - 2.51246 \times 10^{-3} C - 4.02369 \times D + 1.00629 \times 10^{-3} \times A \times B + 0.88733 \times A \times D - 3.22812 \times B \times D \quad (6)$$

Table 1 – ANOVA analysis table for q_e model.

Source	Sum of squares	DF ^a	Mean square	F value ^c	p-Value Prob > F
MS ^b	3.420	8	0.430	91.43	<0.0001
A	0.450	1	0.450	96.64	<0.0001
B	1.500	1	1.500	320.19	<0.0001
C	0.015	1	0.0150	3.210	0.0878
D	0.880	1	0.880	188.32	<0.0001
AB	0.076	1	0.076	16.16	0.0006
AC	0.034	1	0.034	7.170	0.0141
AD	0.072	1	0.072	15.48	0.0008
BD	0.260	1	0.260	55.03	<0.0001
Residual	0.098	21	4.683×10^{-3}		
Cor total	3.520	29			

Where: A: pH; B: concentration (mM); C: temperature (°C) and D: adsorbent dose (g/dm³).

^a Degree of freedom.

^b Model significant.

^c Fisher test: calculated by Model Mean Square divided by Residual Mean Square.

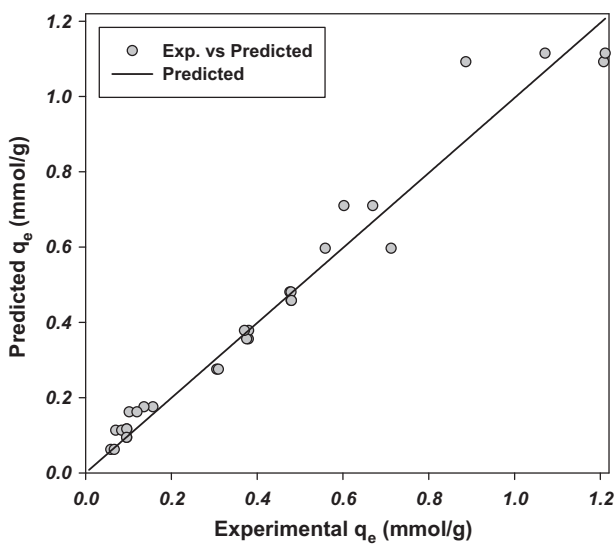


Fig. 1 – Comparison between model prediction and experimental results for q_e .

In Eq. (6) A and B are the initial pH and concentration of the solution respectively, D is the dose (g/dm³) and C is the temperature at which the adsorption experiments are done. The comparison of the model prediction and experimental results is presented in Fig. 1.

Fig. 1 shows a good correlation of the experimental and predicted results. The R^2 value of the fit is 0.9764. The effect of the process variables on the adsorption capacity is summarized by the surface plots shown in Fig. 2(a) and (b). The red colour expressed the optimum conditions at which q_e is maximum. As the q_e value decreases, the colour changes to yellow. Fig. 2(a) shows the effect of initial concentration and dose on the q_e values for three different values of initial pH. Increasing the initial concentration of the solution has the effect of increasing the sorption capacity of the HCO nanoparticles. As can be seen from Fig. 2(a) of the increasing plane gradient, the initial solution pH has a significant effect of reducing the adsorption capacity of the HCO, for temperature of 20 °C and ionic strength of 0.05 M. At lower pH the adsorption capacity is more responsive to changes in the initial concentration hence the steeper gradients. Fig. 2(a) also shows that the Cr(VI) concentration has a greater effect on q_e when compared to dose.

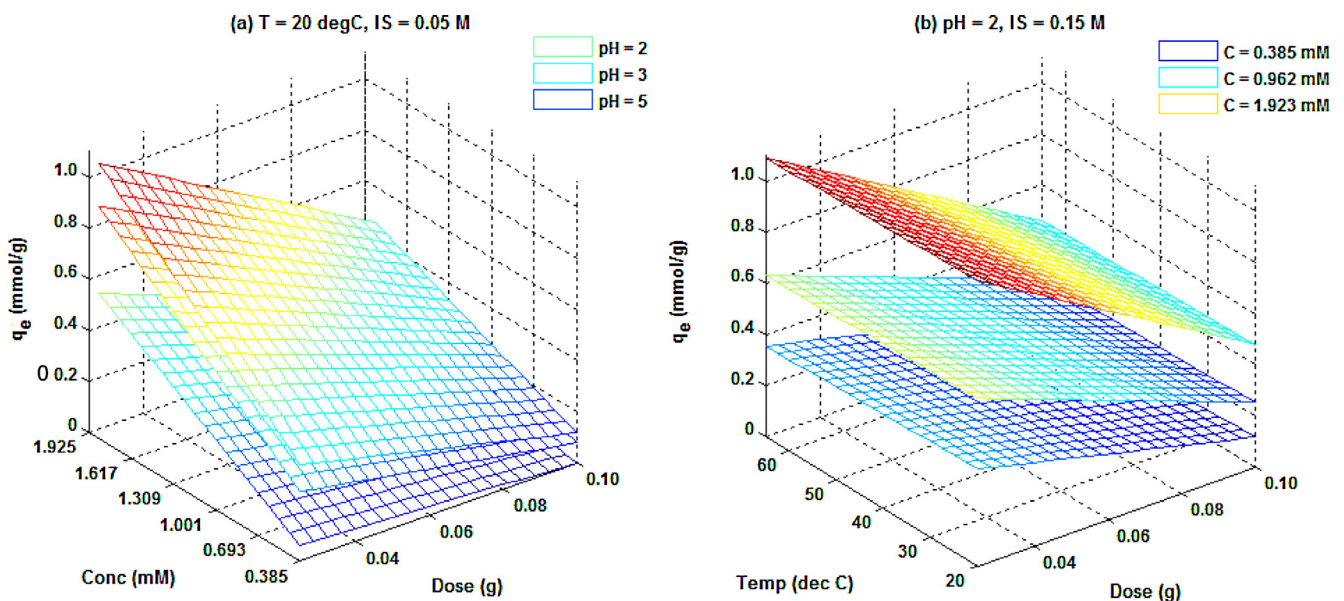


Fig. 2 – Effect of process variables on the q_e (a) effect of concentration, dose and pH (b) effects of temperature, dose and initial concentration.

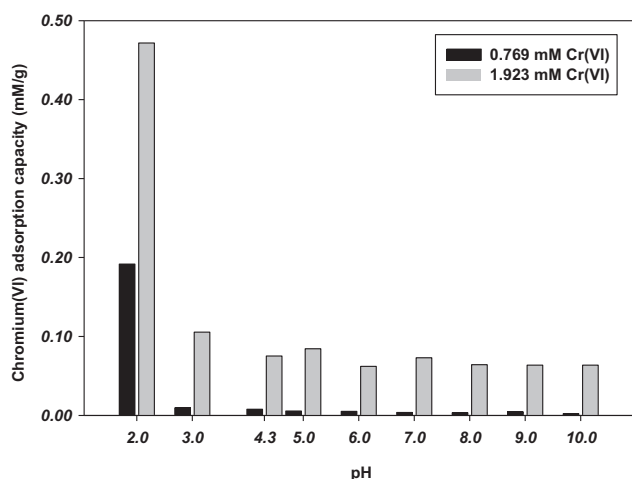


Fig. 3 – Effect of solution pH on Cr(VI) adsorption by hydrous cerium oxide nanoparticles at initial Cr(VI) concentrations 0.769 and 1.923 mM; hydrous cerium oxide dose 4 g/dm³; T = 20 °C.

Higher dosage resulted in more removal of the Cr(VI) from solution, though the q_e values are lower. This is due to the fact that the ions removed from solution are shared among a larger mass of adsorbent, hence lower ion concentration per unit mass of adsorbent. The effect of initial concentration and temperature are further illustrated in Fig. 2(b). Temperature has little effect on the adsorption capacity, as can be seen in Fig. 2(b) where the planes are almost parallel to the temperature axis.

It can be concluded that the main variables affecting the sorption of Cr(VI) are; initial concentration, initial pH of solution and amount of adsorbent used (dose). The detailed discussions of the effect of these variables are presented in the subsequent sections.

3.3. Effect of solution initial pH

The adsorption capability of HCO nanoparticles for the removal of Cr(VI) at initial concentrations $C_0 = 0.769$ mM and 1.923 mM in the single metal sorption system at various pH (2 to 10) is illustrated in Fig. 3. The results clearly indicate that at pH 2, the maximum adsorption capacity of 0.191 and 0.480 mmol/g occurred at an initial Cr(VI) concentration of 0.769 and 1.923 mM, respectively (Fig. 3). At $C_0 = 0.769$, the removal percentage of Cr(VI) decreased drastically from 99.7% to 4.93% and then to 1.09% when pH increased from 2 to 3 and to 10, which is a similar trend to previous reports on Cr(VI) adsorbents (Hu et al., 2011; Yuan et al., 2009).

This shows that the adsorption of the Cr(VI) onto HCO nanoparticles is strongly pH dependent. The increase in Cr(VI) removal efficiency at pH 2 is due, at least in part, to the electrostatic force existing between the sorbent surface and Cr(VI) ions. A strong attraction will exist between these oxyanions of Cr(VI) i.e., HCrO_4^- and the positively charged surface of the adsorbent at low pH (Albadarin et al., 2011a). Whereas, for the pH range 3 to 10, the surface of HCO nanoparticles is negatively charged (IEP at pH 2.7) (Li et al., 2012), and the negative charge increases with the increase of the solution pH. The observed decrease of Cr(VI) adsorption is due to the coulomb repulsive force between the surface of HCO nanoparticles and Cr(VI) ions. This repulsive force increases with an increase in the solution pH from 3 to 10. As discussed in Section 3.1, in

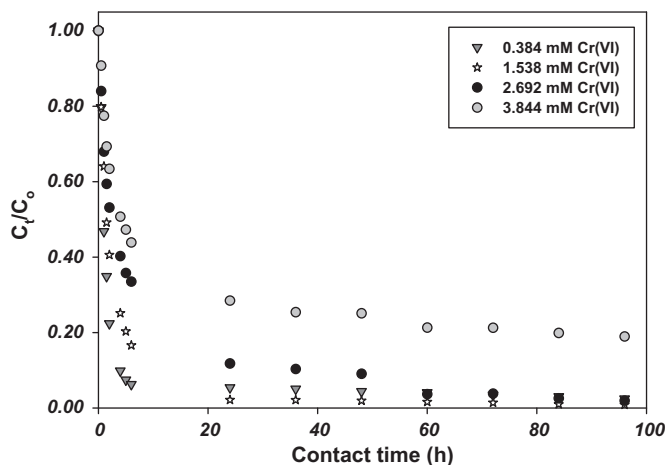


Fig. 4 – Contact times of Cr(VI) adsorption onto hydrous cerium oxide nanoparticles at Cr(VI) concentrations 0.384, 1.538, 2.692, 3.846 mM; shaking time 4 days at 100 rpm; hydrous cerium oxide dose 4 g/dm³; T = 20 °C.

comparison to pH, the ionic strength of the solution had no significant effect on Cr(VI) adsorption. Previous study on the removal of Cr(VI), Albadarin and co-workers (Albadarin et al., 2011a) also showed strong dependency on the pH, but independence of ionic strength. The strong pH dependence and ionic strength independence of Cr(VI) adsorption suggested that surface complexation rather than ion exchange was the dominant mechanism (Du et al., 2012).

3.4. Effect of contact time and initial concentration

The data obtained from the contact time experiment carried out at various concentrations of hexavalent chromium at constant pH 2 are plotted in Fig. 4. In Fig. 4, C_t is the concentration of Cr(VI) at time t . The Cr(VI) removal rate was fast, especially at low concentrations, and the removal gradually reached equilibrium with the increase of treatment time. For instance, about 90% of the Cr(VI) in the solution at $C_0 = 0.384$ mM was adsorbed in just 4 h when the HCO loading was 4 g/dm³. At equilibrium, the percentage uptake of Cr(VI) decreased from 98.7% to 82.3% when the initial Cr(VI) concentration increased from 0.384 to 3.844 mM. Unexpectedly, the percentage removal of Cr(VI) at $C_0 = 1.538$ mM was higher than the percentage removal at $C_0 = 0.384$ mM. This phenomenon is due to the large number of vacant surface sites available for adsorption at low concentration.

With an increase in the initial concentration, the mass transfer driving force would become larger, hence resulting in higher Cr(VI) adsorption. The percentage removal decreases at higher concentrations i.e., 3.844 mM, as the ratio of the initial number of the Cr(VI) ions to the vacant sites is high. However, there does not seem to be much benefit from a contact time longer than 96 h (4 days) for all Cr(VI) initial concentrations. In (Zhang et al., 2003), the TEM images show that the HCO sample is composed of porous powders. Typically, porous solids have low adsorption capacities and act in a kinetically slow manner (Albadarin et al., 2012b). The equilibrium concentration of Cr(VI) was 4.66×10^{-3} mM after the treatment (4 days), which is close to the chromium(VI) MCL suggested by U.S. EPA in inland surface wastewaters (Fruchter, 2002).

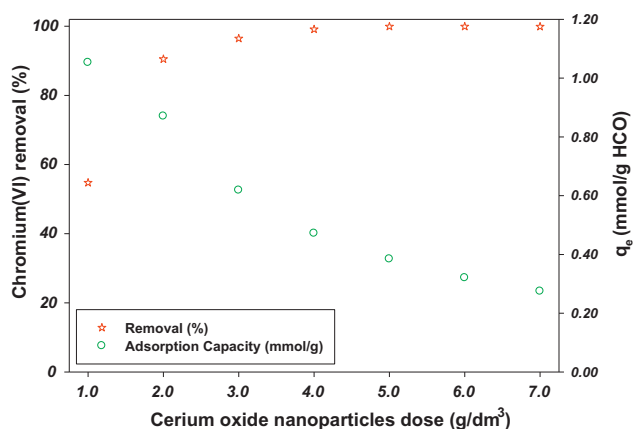


Fig. 5 – Dependence of Cr(VI) ions adsorption on the amount of cerium oxide nanoparticles (HCO).

3.5. Effect of HCO mass–volume ratio

The influence of HCO adsorbent dose on the removal of Cr(VI) at a constant initial Cr(VI) ion concentration of 1.923 mM and pH 2 is illustrated in Fig. 5. It was found that the percentage removal of Cr(VI) increased from 54.7% to 90.6% with an increase in HCO adsorbent dose from 1.0 g/dm³ to 3.0 g/dm³, which is caused by the higher Cr(VI):active site ratio. However, it can be seen that there was no significant change in the percentage removal of Cr(VI) after a dose of 4.0 g/dm³ at which a percentage removal of 98.7% was achieved. Conversely, the decrease in adsorption capacity is due to the splitting effect of the concentration gradient between sorbate and sorbent with increased HCO concentration causing a decrease in the amount of Cr(VI) adsorbed onto a unit weight of HCO (Albadarin et al., 2012b). Typically a point of intersection in this graph is regarded as the optimum dose as this point represents balance between % Cr(VI) removal and adsorption capacity (Dhoble et al., 2011). The intersection point is at 1.52 g/dm³, although, a dose of 4.0 g/dm³ has been selected as it was required to reduce the Cr(VI) levels to near 0.05 mg/dm³ as per EPA guidelines.

3.6. Effect of background ions

Batch equilibrium experiments were carried out to find the individual effect of coexisting anions (SO₄²⁻, PO₄³⁻, Cl⁻, and NO₃⁻) and cations (Ca²⁺ and Mg²⁺) on adsorption of Cr(VI).

The percentage removal of Cr(VI) was compared to samples with no background ions. The results are shown in Fig. 6. Slight decreases of Cr(VI) adsorption were observed when Ca²⁺ and Mg²⁺ cations and Cl⁻ and NO₃⁻ anions coexisted. Cr(VI) adsorption was more significantly decreased from 0.480 mmol/g to 0.115 mmol/g and 0.171 mmol/g when phosphate and sulphate were present, respectively. This decrease in adsorption capacity when phosphate and sulphate coexisted with Cr(VI) in the solution is attributed to their electrostatic interaction and surface complexation onto the hydrous cerium oxide (Dou et al., 2012). This mechanism was also responsible for Cr(VI) removal, so competitive adsorption occurred.

3.7. Adsorption isotherm discussion

The mathematical correlation which establishes a key role for modelling analysis, applicable practice of the adsorption

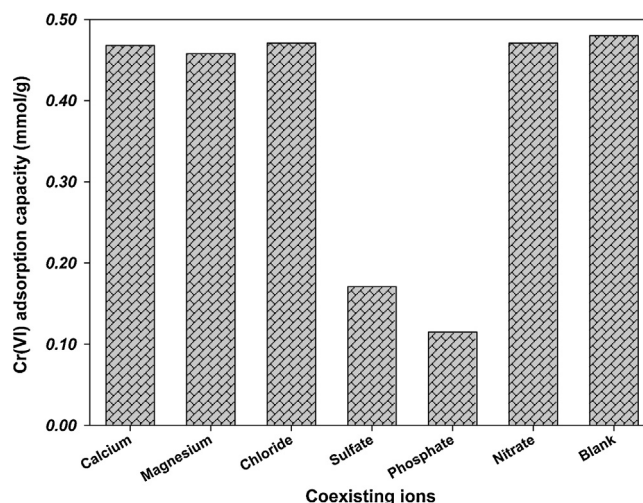


Fig. 6 – Effects of co-existing anions on Cr(VI) removal by HCO.

systems and operational design, is typically resolved by linear regression analysis. However, linear isotherm models have demonstrated to be unable to provide a fundamental understanding of the ion adsorption systems, resulting in improper conclusions (Foo and Hameed, 2012; Ho, 2006). Henceforth, the well-established nonlinear isotherms: the Langmuir (Langmuir, 1916), Freundlich (Freundlich, 1906) and Redlich–Peterson (Redlich and Peterson, 1959) were tested using nonlinear regression.

The Langmuir adsorption isotherm is expressed as (Albadarin et al., 2011b):

$$q_e = q_{\max} \left[\frac{bC_e}{1 + bC_e} \right] \quad (7)$$

The Freundlich isotherm can be expressed in the following form:

$$q_e = K_F C_e^{1/n} \quad (8)$$

The Redlich–Peterson expression can be represented as:

$$q_e = \frac{K_R C_e}{1 + a_R C_e^\beta} \quad (9)$$

where q_{\max} (mmol/g) and b (dm³/mmol) are Langmuir constants related to the capacity and energy of adsorption, respectively. K_F is the Freundlich constant related to the adsorption capacity and can be defined as the adsorption or distribution coefficient and $1/n$ is the heterogeneity factor representing the intensity of adsorption; K_R (dm³/g) a_R and β are the Redlich–Peterson isotherm constants. The isotherms of adsorption were employed using the best experimental conditions previously described. Langmuir and Redlich–Peterson isotherms are the best-fitting isotherms for the experimental results (Fig. 7). The isotherm constants and correlation coefficients of the isotherm models are tabulated in Table 2. As can be observed, the value of β constant was close to unity (0.990), which means that the Redlich–Peterson isotherm is approaching the Langmuir form and not the Freundlich isotherm. Conformation of the data into the Langmuir isotherm model demonstrated the formation of monolayer coverage of Cr(VI) at the outer surface of HCO and showed the homogeneous nature of Cr(VI) adsorption onto HCO which suggests that adsorption sites are identical and

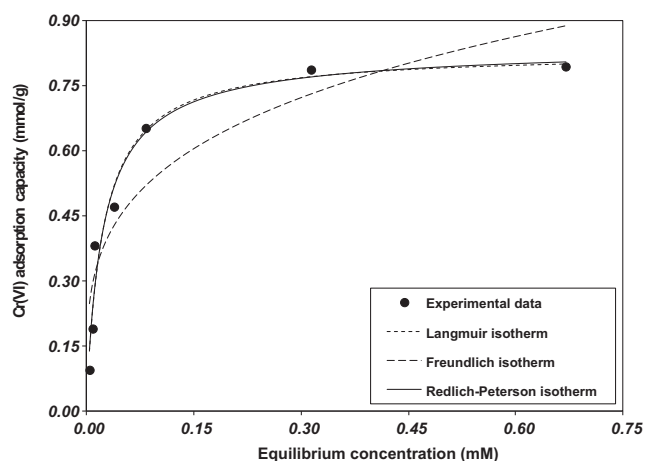


Fig. 7 – Adsorption isotherm for Cr(VI) by the hydrous cerium oxide with a suspension dose of 4 g/dm³ at pH 2, initial Cr(VI) concentrations 0.384–3.846 mM and exposure time: 96 h at 20 °C.

energetically equivalent (Langmuir, 1916). Similar conclusions were obtained for the adsorption of phosphate (Huichao Guo et al., 2011), As(V) (Li et al., 2012) and fluoride (Guo et al., 2011) onto hydrous cerium oxide. The maximum adsorption capacity of Cr(VI) onto hydrous cerium oxide in this study is higher than that for the magnetic iron–nickel oxide (30 mg/g) (Wei et al., 2009) and magnetite nanoparticles (20.16 mg/g) and lower than that for iron (Fe³⁺) oxide/hydroxide nanoparticles (87.30 mg/g) (Zelmanov and Semiat, 2011).

3.8. Influence of different desorbents

In order to determine the possibility of re-using the HCO as an adsorbent for the adsorption of Cr(VI) ions, desorption experiments were carried out. NaOH, H₂SO₄ and HCl aqueous solutions (0.1–1.0 M) and deionised water were tested for regeneration of the loaded adsorbent. The time course required for the efficient release of bound Cr(VI) ions was monitored as 6 h, by which the time adsorbed ions were almost completely eluted. The recovery using deionised water did not occur efficiently even after 12 h of agitation (recovery <1%). As can be seen in Fig. 8 the recovery of the adsorbent using aqueous NaOH and H₂SO₄ of different concentrations as regenerating solutions occurred efficiently. The best elution efficiency was obtained using NaOH 0.1 M solution (~85%). The desorption results indicate that the Cr(VI) adsorption on the hydrous cerium oxide (HCO) is not completely reversible and

Table 2 – Langmuir, Freundlich and Redlich–Peterson isotherm constants and regression correlation coefficients for the adsorption of Cr(VI) onto HCO.

Isotherm	Parameters	Value
Langmuir isotherm model	q_{\max} (mmol/g)	0.828
	b (dm ³ /mmol)	43.02
	R^2	0.963
Freundlich isotherm model	K_F (mmol/g)(mM) ^{1/n}	0.984
	$1/n$	0.257
	R^2	0.849
Redlich–Peterson isotherm model	K_R	36.80
	a_R	44.04
	β	0.990
	R^2	0.963

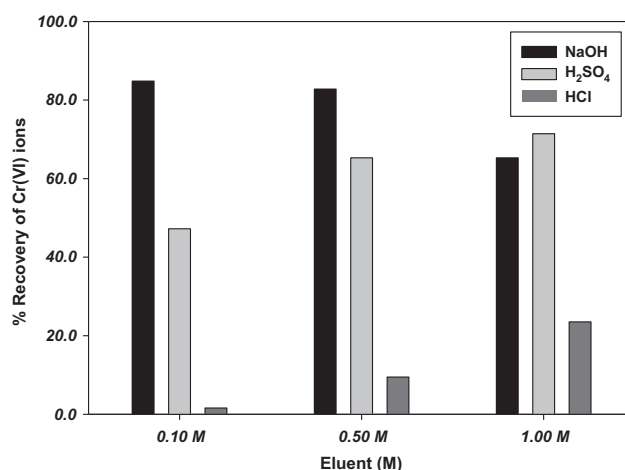


Fig. 8 – Desorption of Cr(VI) loaded on HCO using various desorbents.

Cr(VI) can be desorbed from the HCO nanoparticles surface by altering the pH values of the solution. Complete desorption was not possible which is attributed to the involvement of non-electrostatic forces between the HCO and the Cr(VI) ions. Effects of pH and desorption studies indicate that chemisorption and ion exchange mechanisms are functioning within the adsorption process. Hydrous cerium oxide–Cr(VI) complex formation ($\equiv\text{HCO}-\text{OH}^+-\text{HCrO}_4^-$) is chemisorption. It can be assumed that, only the Cr(VI) ions that are adsorbed by ion-exchange are desorbed and the Cr(VI) ions that are removed by complex formation are not desorbed (Rodrigues et al., 2010).

3.9. FTIR analysis

The Cr(VI) adsorption mechanism was investigated with the microscopic technique of FTIR spectroscopy. Fig. 9 shows the FTIR spectra of HCO before adsorption and the Cr(VI)–HCO nanoparticles after adsorption. The FTIR spectrum of HCO nanoparticles shows a broad absorption peak corresponding to OH⁻ stretching (3300–3500 cm⁻¹) and bending vibrations (1789 cm⁻¹). This indicates the presence of hydroxyl groups on the surface of the HCO nanoparticles (or it may be due to the adsorption of some atmospheric water during FTIR measurements). Bending vibrations of hydroxyl groups on Ce–OH at 1147 and 1067 cm⁻¹ (Zhang et al., 2005) and NO₃⁻ vibrations

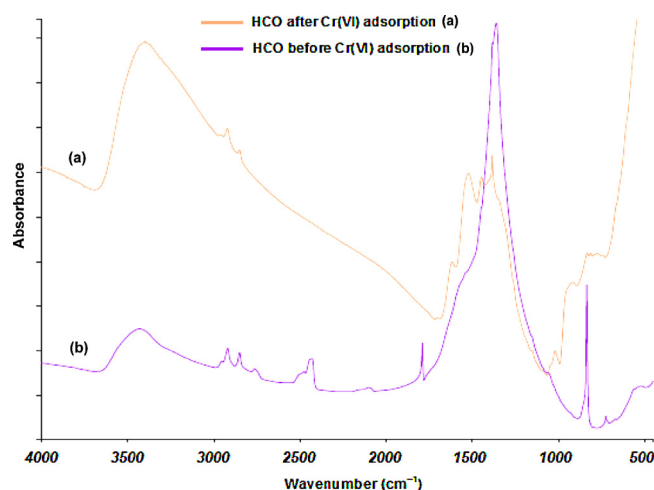


Fig. 9 – FTIR spectra for HCO nanoparticles before and after Cr(VI) adsorption.

at 1361 cm^{-1} are attributed to the residue from $\text{Ce}(\text{NO}_3)_3 \cdot 6\text{H}_2\text{O}$ used in the adsorbent preparation. The peaks in the range of $2921\text{--}2765\text{ cm}^{-1}$ correspond to the C–H stretch vibration, which may come from the surface of the tubes or the ethanol residue. After adsorption, the FTIR spectrum of Cr(VI)–HCO nanoparticles shows that peaks at 1147 cm^{-1} , 1067 cm^{-1} and 837 cm^{-1} almost disappear and the peak at 1361 cm^{-1} was shifted and reduced. New peaks at 1515 , 994 and 892 cm^{-1} which are caused by the formation of a Ce–O–Cr bond, are indicative of the formation of inner-sphere complexes on Cr(VI)–HCO nanoparticles (Guan et al., 2008). This is in agreement with previous discussion in sections on the pH effect. This confirms that the dominant Cr(VI) adsorption mechanism by HCO nanoparticles was surface complexation with the formation of an inner-sphere complex.

4. Conclusions

Hydrous cerium oxide (HCO) is a promising adsorbent for the removal of Cr(VI) from aqueous systems. From the factorial experimental design, the optimum conditions for the best adsorption results are: 1.923 mmol/g of Cr(VI) metal concentration, pH 2, temperature 20°C and a sorbent dose of 4 g/dm^3 after 96 h contact time. A significant decline in Cr(VI) adsorption occurred when the pH was higher than 2 due to the electrostatic repulsion between the Cr(VI) ions and the HCO nanoparticle surface. The ionic strength independence of Cr(VI) adsorption shows that the ion exchange mechanism is not the main adsorption mechanism. The coexisting anions, especially sulphate and phosphate, influenced the adsorption capacity as a result of the competitive adsorption. The experimental data fits the Langmuir isotherm better than the Freundlich isotherm. The significant capacity of HCO adsorbent to remove the Cr(VI) and the applicability in desorbing the Cr(VI) ions using 0.1 M NaOH solution, make HCO nanoparticles a promising material for the efficient removal of toxic Cr(VI) from the wastewater.

References

- Duffy, A., Walker, G.M., Allen, S.J., 2006. Investigations on the adsorption of acidic gases using activated dolomite. *Chemical Engineering Journal* 117, 239–244.
- Fendorf, S.E., 1995. Surface reaction of chromium in soils and waters. *Geoderma* 67, 55–71.
- Kotas, J., Stasicka, Z., 2000. Chromium occurrence in the environment and methods of its speciation. *Environmental Pollution* 107, 263–283.
- Albadarin, A.B., Mangwandi, C., Walker, G.M., Allen, S.J., Ahmad, M.N.M., Khraisheh, M., 2012a. Influence of solution chemistry on Cr(VI) reduction and complexation onto date-pits/tea-waste biomaterials. *Journal of Environmental Management* 114, 190–201.
- Zou, J., Wang, M., Jiang, W., Liu, D., 2006. Chromium accumulation and its effects on other mineral elements in *amaranthus viridis* L. *Acta Biologica Cracoviensia: Series Botanica* 48, 7–12.
- Iskanska, A., Gładysz, P., Majdan, M., Pikus, S., Sternik, D., 2012. Simultaneous adsorption of chromium(VI) and phenol on natural red clay modified by HDTMA. *Chemical Engineering Journal* 179, 140–150.
- Albadarin, A.B., Mangwandi, C., Al-Muhtaseb, A.A.H., Walker, G.M., Allen, S.J., Ahmad, M.N.M., 2012b. Kinetic and thermodynamics of chromium ions adsorption onto low-cost dolomite adsorbent. *Chemical Engineering Journal* 179, 193–202.
- McCarroll, N., Keshava, N., Chen, J., Akerman, G., Kligerman, A., Rinde, E., 2010. An evaluation of the mode of action framework for mutagenic carcinogens case study II: chromium (VI). *Environmental and Molecular Mutagenesis* 51, 89–111.
- Santhana Krishna Kumar, A., Gupta, T., Kakan, S.S., Kalidhasan, S., Manasi, Rajesh, V., Rajesh, N., 2012. Effective adsorption of hexavalent chromium through a three center (3c) co-operative interaction with an ionic liquid and biopolymer. *Journal of Hazardous Materials* 239–240, 213–224.
- Recillas, S., Colón, J., Casals, E., González, E., Puentes, V., Sánchez, A., Font, X., 2010. Chromium VI adsorption on cerium oxide nanoparticles and morphology changes during the process. *Journal of Hazardous Materials* 184, 425–431.
- Al-Degs, Y.S., El-Sheikh, A.H., Al-Ghouti, M.A., Hemmateenejad, B., Walker, G.M., 2008. Solid-phase extraction and simultaneous determination of trace amounts of sulphonated and azo sulphonated dyes using microemulsion-modified-zeolite and multivariate calibration. *Talanta* 75, 904–915.
- Jabeen, H., Chandra, V., Jung, S., Lee, J.W., Kim, S.B.K.S., 2011. Enhanced Cr(VI) removal using iron nanoparticle decorated grapheme. *Nanoscale* 3, 3583–3585.
- Xiao, H., Ai, Z., Zhang, L., 2009. Nonaqueous sol-gel synthesized hierarchical CeO_2 nanocrystal microspheres as novel adsorbents for wastewater treatment. *Journal of Physical Chemistry C* 113, 16625–16630.
- Yuan, P., Liu, D., Fan, M., Yang, D., Zhu, R., Ge, F., Zhu, J., He, H., 2010. Removal of hexavalent chromium [Cr(VI)] from aqueous solutions by the diatomite-supported/unsupported magnetite nanoparticles. *Journal of Hazardous Materials* 173, 614–621.
- Li, R., Li, Q., Gao, S., Shang, J.K., 2012. Exceptional arsenic adsorption performance of hydrous cerium oxide nanoparticles: part A. Adsorption capacity and mechanism. *Chemical Engineering Journal* 185–186, 127–135.
- Raichur, A.M., Jyoti Basu, M., 2001. Adsorption of fluoride onto mixed rare earth oxides. *Separation and Purification Technology* 24, 121–127.
- Duranoğlu, D., Trochimczuk, A.W., Beker, U., 2012. Kinetics and thermodynamics of hexavalent chromium adsorption onto activated carbon derived from acrylonitrile-divinylbenzene copolymer. *Chemical Engineering Journal* 187, 193–202.
- Zhang, Y.-W., Si, R., Liao, C.-S., Yan, C.-H., 2003. Facile alcoholthermal synthesis, size-dependent ultraviolet absorption, and enhanced CO conversion activity of ceria nanocrystals. *Journal of Physical Chemistry B* 107, 10159–10167.
- Tel, H., Altas, Y.T.M.S., 2004. Adsorption characteristics and separation of Cr(III) and Cr(VI) on hydrous titanium(IV) oxide. *Journal of Hazardous Materials* B112, 225–231.
- Álvarez-Ayuso, E., García-Sánchez, A., Querol, X., 2007. Adsorption of Cr(VI) from synthetic solutions and electroplating wastewaters on amorphous aluminium oxide. *Journal of Hazardous Materials* 142, 191–198.
- Hu, X.-J., Wang, J.-S., Liu, Y.-G., Li, X., Zeng, G.-M., Bao, Z.-L., Zeng, X.-X., Chen, A.-W., Long, F., 2011. Adsorption of chromium (VI) by ethylenediamine-modified cross-linked magnetic chitosan resin: isotherms, kinetics and thermodynamics. *Journal of Hazardous Materials* 185, 306–314.
- Yuan, P., Fan, M., Yang, D., He, H., Liu, D., Yuan, A., Zhu, J., Chen, T., 2009. Montmorillonite-supported magnetite nanoparticles for the removal of hexavalent chromium [Cr(VI)] from aqueous solutions. *Journal of Hazardous Materials* 166, 821–829.
- Albadarin, A.B., Al-Muhtaseb, A.A.H., Walker, G.M., Allen, S.J., Ahmad, M.N.M., 2011a. Retention of toxic chromium from aqueous phase by H_3PO_4 -activated lignin: effect of salts and desorption studies. *Desalination* 274, 64–73.
- Du, G., Li, Z., Liao, L., Hanson, R., Leick, S., Hoepfner, N., Jiang, W.-T., 2012. Cr(VI) retention and transport through Fe(III)-coated natural zeolite. *Journal of Hazardous Materials* 221–222, 118–123.
- Fruchter, J., 2002. In-situ treatment of chromium-contaminated groundwater. *Environmental Science and Technology* 23, 464–472.
- Dhoble, R.M., Lunge, S., Bhole, A.G., Rayalu, S., 2011. Magnetic binary oxide particles (MBOP): a promising adsorbent for

- removal of As (III) in water. *Water Research* 45, 4769–4781.
- Dou, X., Mohan, D., Pittman Jr., C.U., Yang, S., 2012. Remediating fluoride from water using hydrous zirconium oxide. *Chemical Engineering Journal* 198–199, 236–245.
- Foo, K.Y., Hameed, B.H., 2012. Microwave-assisted preparation and adsorption performance of activated carbon from biodiesel industry solid residue: influence of operational parameters. *Bioresource Technology* 103, 398–404.
- Ho, Y.-S., 2006. Isotherms for the sorption of lead onto peat: comparison of linear and non-linear methods. *Polish Journal of Environmental Studies* 15, 81–86.
- Langmuir, I., 1916. The constitution and fundamental properties of solids and liquids. *Journal of the American Chemical Society* 38, 2221–2295.
- Freundlich, H., 1906. Über die adsorption in lösungen (adsorption in solution). *Zeitschrift für Physikalische Chemie* 57, 384–470.
- Redlich, O., Peterson, D.L., 1959. A useful adsorption isotherm. *Journal of Physical Chemistry* 63, 1024–1026.
- Albadarin, A.B., Chirangano Mangwandi, Walker, Gavin M., Allen, S.J., Ahmad, M.N., 2011b. Biosorption characteristics of sawdust for the removal of Cd(II) ions: mechanism and thermodynamic studies. *Chemical Engineering Transactions* 24, 1297–1302.
- Guo, H., Li, W., Wang, H., Zhang, J., Liu, Y., Zhou, Y., 2011. A study of phosphate adsorption by different temperature treated hydrous cerium oxides. *Rare Metals* 30, 58–62.
- Guo, H.C., Li, W.J., Chang, Z.D., Wang, H.Y.Z.Y., 2011. Mechanism study of fluoride adsorption by hydrous metal oxides. *PubMed PMID: 22007419* 8, 2210–2214.
- Wei, L., Yang, G., Wang, R., Ma, W., 2009. Selective adsorption and separation of chromium (VI) on the magnetic iron–nickel oxide from waste nickel liquid. *Journal of Hazardous Materials* 164, 1159–1163.
- Zelmanov, G., Semiat, R., 2011. Iron (Fe³⁺) oxide/hydroxide nanoparticles-based agglomerates suspension as adsorbent for chromium (Cr⁶⁺) removal from water and recovery. *Separation and Purification Technology* 80, 330–337.
- Rodrigues, L.A., Maschio, L.J., da Silva, R.E., da Silva, M.L.C.P., 2010. Adsorption of Cr(VI) from aqueous solution by hydrous zirconium oxide. *Journal of Hazardous Materials* 173, 630–636.
- Zhang, Y., Yang, M., Dou, X.-M., He, H., Wang, D.-S., 2005. Arsenate adsorption on a Fe–Ce bimetal oxide adsorbent: role of surface properties. *Environmental Science and Technology* 39, 7246–7253.
- Guan, X.-H., Wang, J., Chusuei, C.C., 2008. Removal of arsenic from water using granular ferric hydroxide: macroscopic and microscopic studies. *Journal of Hazardous Materials* 156, 178–185.